DR. JEREMÍAS GASTÓN GALLETTI (Orcid ID : 0000-0002-5118-2540)

Article type : Original Article

Title: **Transient tear hyperosmolarity disrupts the neuroimmune homeostasis of the ocular surface and facilitates dry eye onset**

Authors: Mauricio Guzmán, Maximiliano Miglio, Irene Keitelman, Carolina Maiumi Shiromizu, Florencia Sabbione, Federico Fuentes, Analía S Trevani, Mirta N Giordano, Jeremías G Galletti

Affiliations: Laboratorio de Inmunidad Innata, Instituto de Medicina Experimental, Academia Nacional de Medicina/CONICET, Buenos Aires, Argentina

Corresponding author: Jeremías G. Galletti
email: jeremiasg@gmx.net
phone: +54 (11) 4823 1189

Mailing address: Pacheco de Melo 3081
(1425) Buenos Aires, Argentina.

Running head: Hyperosmolarity's role in dry eye

Keywords: dry eye, hyperosmolar stress, tear hyperosmolarity, transient receptor potential vanilloid 1, ocular mucosal tolerance

There is no conflict of interest for all the authors.

Abbreviations: DED: dry eye disease, PBS: phosphate-buffered saline, OVA: ovalbumin, THO: tear hyperosmolarity, DTH: delayed type-hypersensitivity, NF-κB: nuclear factor-κB, DC: dendritic cell, TRPV1: transient receptor potential vanilloid channel type 1, MAPK: mitogen-activated protein kinase

Summary

Dry eye disease (DED) is a highly prevalent ocular surface disorder with neuroimmune pathophysiology. Tear hyperosmolarity (THO), a frequent finding in affected patients, is considered a key element in DED pathogenesis, yet existing animal models are based on subjecting the ocular surface to the more complex desiccating stress -decreased tear production and/or increased evaporation- instead of strict hyperosmolar stress. Here we characterized a murine model of THO that does not involve desiccating stress, thus allowing us to dissect the contribution of THO to DED. Our results showed that tear hyperosmolarity (THO) is sufficient to disrupt neuroimmune homeostasis of the ocular surface in mice, and thus reproduce many subclinical DED findings. THO activated nuclear factor-κB signaling in conjunctival epithelial cells and increased dendritic cell recruitment and maturation, leading to more activated (CD69+) and memory (CD62lo CD44hi) CD4+ T cells in the eye-draining lymph nodes. Ultimately, THO impaired the development of ocular mucosal tolerance to a topical surrogate antigen in a chain of events that included epithelial nuclear factor-κB signaling and activation of transient receptor potential vanilloid 1 as the probable hypertonicity sensor. Also, THO reduced the density of corneal intraepithelial nerves and terminals and sensitized the ocular surface to hypertonicity. Finally, the adoptive transfer of T cells from THO mice to naïve recipients under mild desiccating stress favored DED development, showing that THO is enough to trigger an actual pathogenic T cell response. Our results altogether demonstrate that THO is a critical initiating factor in DED development.

Introduction

Dry eye disease (DED) is a highly prevalent, multifactorial disorder of the ocular surface that can considerably impair quality of life(1). Both inflammation and neuropathic pain play a role in DED pathophysiology, but the extent to which each of the two contributes to clinical signs and symptoms varies markedly from patient to patient. Among clinical findings, tear hyperosmolarity (THO), i.e. tear osmolarity above the physiological range (302±9.7 mOsm/l)(2), is frequently detected and correlates well with disease severity(3). THO can result from low aqueous tear production and/or increased tear evaporation, and it is considered a core driver in DED pathophysiology, causing inflammation and ocular surface damage(4,5). However, it is unclear whether THO arises early in the course of the disease or if it is a manifestation of tear film dysfunction once the vicious cycle of DED is established(4).

A large body of evidence shows that hyperosmolar stress reproduces on cultured corneal epithelial cells many of the findings of DED(6–9), and at least some corresponding early responses to hyperosmolar stress have been reported in the ocular surface epithelia of mice(5). Interestingly, many new cases of DED are linked to video display or smartphone use, which leads to reduced blinking frequency and more incomplete blinks, and thus more tear evaporation and the consequent THO(1,10–13). Vocational video display users but not age-matched non-video display users have increased tear osmolarity at the end of the work day(13). Although aging is the strongest risk factor for DED in population-wide studies(1), these new patients are considerably younger than the overall DED population and have normal lacrimal function and no systemic comorbidities(14). Therefore, transient exposure to THO during video display or smartphone use could be the sole initiating factor in these patients(1,14). Nonetheless, it remains to be determined whether THO is enough to disrupt the homeostatic mechanisms of the ocular surface that prevent the onset of the pathogenic Th1/Th17 immune response(15,16), and thus the vicious cycle of DED(4).

The ocular surface is a tightly regulated mucosal lining: despite being continuously exposed to harmless environmental antigens, it remains uninflamed and thus fit for sight purposes under normal circumstances. This is so because a set of homeostatic mechanisms prevent unwanted, potentially damaging inflammation from arising in response to challenges that do not pose a threat(17). This

phenomenon is experimentally known as mucosal tolerance and involves the generation of antigen-specific regulatory T cells that suppress inflammation(17–19). Loss of ocular mucosal tolerance (and thus, of mucosal immune homeostasis) has been implicated in other ocular inflammatory disorders such as eye drop preservative toxicity(19) and allergic conjunctivitis(20). Moreover, we have previously shown that in conventional murine models of DED, a disruption in ocular mucosal tolerance eventually ensues and contributes to ocular surface damage(21,22). In these DED models, desiccating stress is a prerequisite for mucosal tolerance breakdown, but the exact initiating factor in the context of ocular surface desiccation is unknown. THO due to increased evaporation is a necessary component of desiccating stress but not the only one, as desiccation and hypertonic stress induce different gene expression responses in human cells(23).

Interestingly, some DED patients exhibit little or no ocular surface findings yet they report pain or ocular dysesthesia, which could be regarded as a neuropathic presentation of the disease(24). In line with the neuropathic etiology, corneal nerve abnormalities and altered corneal sensitivity have been described in these patients(24–26). Besides, the cornea is densely innervated, and regulatory neuroimmune crosstalk is crucial for ocular surface homeostasis(27–29). Corneal intraepithelial nerves terminate as free nerve endings interspersed between the apical squamous epithelial cells, almost in direct contact with the tear film(30). In a DED model, desiccating stress rapidly induces a break in the apical corneal epithelial barrier(31), along with structural and functional alterations in corneal intraepithelial nerves(32,33). Given these observations, increased exposure of the corneal intraepithelial nerves to the abnormal tear film might be responsible for the aforementioned changes, which in turn also play a role in DED pathophysiology.

Considering its prevalence in DED, we hypothesized that THO could have a role in initiating the disruption in ocular surface immune homeostasis and the corneal nerve alterations that underlie the different presentations of DED. Therefore, we set out to explore these possibilities in a murine model of THO without desiccating stress, to better understand the contribution of hyperosmolar stress to the onset of DED.

Results

THO disrupts mucosal immune homeostasis of the ocular surface

In order to test the effect of THO on ocular mucosal tolerance, we modified the model of THO-induced ocular surface inflammation from Luo et al(5), who applied 500 mOsm/l saline six times a day for two days on both eyes of mice and found increased production of DED-associated pro-inflammatory factors. Instead, we instilled both eyes of Balb/c mice four times daily for five days with two different concentrations of hyperosmolar saline or iso-osmolar saline (300 mOsm/l) as control. The selection of the conditions was based on the following observations. First, the accepted physiological range for tear osmolarity (302±9.7 mOsm/l) and the reported 5-10% increase in DED come from sampling the lower tear meniscus(2,34), where osmolarity is lower than in the precorneal tear film, especially in DED(35). Modeling of THO is complicated by the fact that the tear film is neither spatially uniform (being thinnest on the central cornea, ~2 μm thick)(36) nor temporally (due to the blink cycle). Also, instillation of 800-900 mOsm/l saline in humans is necessary to elicit symptoms comparable to those of DED(37), and mathematical modeling predicts spikes of 1900 mOsm/l and even 3000 mOsm/l under the worst conditions (maximum evaporation due to prolonged blinking intervals)(4,38). Therefore, to accommodate these observations within our murine model we tested two different hyperosmolar treatments (900 and 3000 mOsm/l, or 0.9 and 3 Osm/l, respectively). It should be noted that during each instillation, the ocular surface was exposed briefly to said hyperosmolarity due to dilution of the instilled solution in the tear film and more importantly, because of the reflex tearing that was induced by the hyperosmolar stimulus.

Since the antigen specificity of the T cells responsible for corneal damage in DED is unknown(17), we imbibed the eyes with an inert exogenous protein, ovalbumin (OVA), to serve as a surrogate ocular surface antigen that allowed us to track the antigen-specific immune response. Under non-DED conditions, mice exposed to OVA eye drops develop OVA-specific regulatory T cells that reduce subsequent immunization with the same antigen. This homeostatic mechanism is termed mucosal tolerance because it prevents unwanted inflammation against the harmless foreign antigens to which mucosal linings are continuously exposed(17,39). We have previously observed that mice must be exposed to desiccating stress over three days before they lose ocular mucosal tolerance to

OVA(21,22), that is, they develop OVA-specific effector T cells instead of regulatory T cells. Therefore, in this setup, we also deferred the instillation of OVA by three days to allow for a potentially similar disruptive effect to take place but induced instead by THO (Figure 1A). As readouts for antigen-specific T cell responses, we measured in vivo delayed type-hypersensitivity (DTH) responses and in vitro OVA-induced T cell proliferation. As expected, mice that were not previously exposed to OVA showed full-blown DTH responses (Figure 1B) and high T cell proliferation (Figure 1C), whereas mice instilled with isoosmolar saline (0.3 Osm/l) and later exposed to OVA developed blunted DTH responses and lower T cell proliferation (Figures 1B and 1C, evidence of mucosal tolerance). By contrast, mice exposed first to THO and then to OVA had full DTH responses and high T cell proliferation, that is, lack of mucosal tolerance (Figures 1B and 1C). As instillation of 3 Osm/l saline produced more consistent results than 0.9 Osm/l saline for THO treatment, we selected the higher concentration for the remaining experiments (referred to as THO mice). The chosen osmolarity is comparable to that of over-the-counter available eye drops (5% NaCl) approved for temporary relief of corneal edema in humans, and to the peak values calculated for the exposed ocular surface(4,38). Confirming the observed difference in T cell responses, increased numbers of activated ($CD69^{+}$) and memory ($CD62L^{lo}$ $CD44^{hi}$) CD4+ T cells were detectable on day 5 of instillation in the draining lymph nodes of THO mice (Figure 1D). We also observed more CD8+ CD103+ T cells in the draining lymph nodes of THO mice at this time point (Figure 1D), a finding consistent with what has been reported in a murine DED model(40). These CD8+ T cells increase in number in the lymph nodes during desiccating stress, and they exert a regulatory role as their depletion worsens DED in mice(40). Altogether these findings show that THO in and of itself is sufficient to disrupt ocular surface immune tolerance, as previously reported for desiccating stress in DED models(21,22).

THO alters the ocular surface immune microenvironment

Since we observed that THO was sufficient to disrupt mucosal tolerance in mice similarly to desiccating stress, we then examined its effect on the conjunctival epithelium and dendritic cells (DCs). First, we assessed the activation status of the nuclear factor (NF)-κB pathway in conjunctival epithelial cells, as this transcription factor has been shown to govern the type of mucosal immune response (tolerogenic vs immunogenic)(41,42). A higher level of NF-κB activation was detected in

conjunctival epithelial cells from mice exposed to THO for 3 days (Figure 2A), and in line with the aforementioned functional role, instillation of pyrrolidine dithiocarbamate -an NF-κB inhibitor-, abrogated the disruptive effect of hyperosmolar stress on ocular mucosal tolerance (Figure 2B). Then, we looked at ocular surface DCs, as these antigen-presenting cells are conditioned by ocular surface epithelial cells and are critical in DED progression(43). There were more conjunctival DCs in THO mice (Figures 2C), in agreement with what has been reported for corneal and conjunctival DC numbers in a murine DED model(44) and DED patients(45–47). Also, we observed a larger tree area (Figures 2D) and more dendrites (Figures 2E) in the conjunctival DCs in THO mice, two findings indicative of increased activation(46). To corroborate these indirect signs of dendritic cell maturation, we explored the functional effect of THO on ocular surface DCs. To this aim, we modified the experimental setup to allow for conditioning of the ocular surface microenvironment by performing only iso- or hyperosmolar saline instillation for three days and then injecting immature DCs that were either loaded with OVA in vitro or derived from an allogeneic mouse. Thus, once injected in the subconjunctival space, the DCs received local conditioning signals that modified their antigen presentation capacity before migrating to the eye-draining lymph nodes and presenting a foreign antigen to naïve T cells. As shown in Figures 2F and 2G, THO mice that received either allogeneic immature DCs or syngeneic immature DCs loaded with OVA exhibited greater antigen-specific T cell responses upon in vivo or in vitro challenge, showing that THO favored immunogenic instead of tolerogenic conditioning of locally transferred DCs. This result is consistent with the increased DC maturation that has been observed in the eye-draining lymph nodes of DED mice(48). We confirmed the effect of THO on conjunctival antigen presentation by transferring CD4+ cells from OVA-specific T cell receptor transgenic mice (DO11.10) to naïve wild-type recipients that also received either iso- or hyperosmolar saline instillation. After two days, these mice were instilled OVA in addition to saline. As shown in Figure 2H, there were more DO11.10+ CD4+ cells in the eye-draining lymph nodes of THO mice than of control mice, suggesting that more efficient antigen presentation was taking place in THO mice, as is also the case for DED mice(48). Finally, we explored the potential role of a THO sensor in this hyperosmolar stress-induced immune disruption model. Hypertonicity induces activation of the transient receptor potential vanilloid channel type 1 (TRPV1) signaling pathway in corneal epithelial cells(49,50), which ultimately results in NF-κB activation. Moreover,

we have previously shown that this receptor is involved in another model of ocular surface immune disruption(27). Therefore, we tested its role in THO signaling by adding the instillation of a TRPV1 antagonist along with hypertonic saline. As shown in Figure 2I, topical TRPV1 blockade did not affect homeostatic ocular mucosal tolerance in control mice, but it did prevent the development of an effector T cell response to OVA in THO mice. In other words, ocular TRPV1 blockade abrogated the disruptive effect of THO on ocular mucosal tolerance. These findings show that hyperosmolar stress activates ocular surface epithelial cells and DCs, and that TRPV1 signaling is involved in this process.

Given the changes induced by THO in ocular surface epithelial cells and DCs, we then examined its effect on corneal intraepithelial nerves, as they lie closely and interact extensively with epithelial cells and DCs. We detected a drop in intraepithelial nerve terminals in the corneas of mice under THO for five days (Figure 3A), as well as a decrease in subbasal nerve fibers in the central and peripheral cornea as evidenced by Sholl analysis (Figure 3B) and total sum length (Figure 3C), respectively. Of note, comparable effects have been reported in DED mice(32). Since DED is associated with corneal nerve sensitization(51), we also tested the blinking response in mice exposed to THO for five days. THO mice blinked more in response to a hyperosmolar stimulus (Figure 3D), suggesting that the anatomical changes in the nerves were accompanied by a modification in the physiological response.

Altogether these results show that hyperosmolar stress induces changes in conjunctival epithelial cells and DCs, setting the stage for immunogenic antigen presentation, and also in corneal nerves, potentially affecting homeostatic neuroimmune crosstalk.

THO does not induce corneal damage per se but initiates a T cell response that favors DED development

Since we readily observed a change in the ocular surface mucosal immune response of mice under THO, we examined their eyes for clinical signs of DED. Contrasting the stark changes in ocular mucosal immune homeostasis, mice under THO for five days showed no difference in tear production (Figure 4A), corneal fluorescent staining (a clinical outcome measurement for corneal epithelial damage, Figure 4B) and corneal irregularity (a surrogate outcome for corneal epithelial damage, Figure 4C). Thus, corneal findings were markedly different from what we and others have previously

observed in conventional desiccating stress DED models, which develop considerable corneal epithelial damage over five days(15,16,21,22,52).

Given both the profound changes in the ocular mucosal immune response and the lack of clinical ocular surface disease signs in THO mice, we hypothesized that THO might facilitate DED onset. Thus, we tested if T cells expanded in vivo in mice subjected to hyperosmolar stress for five days were able to reproduce DED signs under suboptimal environmental conditions, i.e. insufficient to induce the disease in naïve recipient mice. To this aim (Figure 5A), we adoptively transferred the CD3+ T cells from spleens and lymph nodes of control or THO mice to recipients that were subsequently exposed to mild desiccating stress (forced airflow without scopolamine). Recipients were depleted of regulatory T cells by CD25 antibody treatment prior to transfer because it has been shown that these cells prevent the development of DED phenotype in Balb/c mice transferred with pathogenic T cells(52). As shown in Figure 5B, CD4+ and CD8+ T cells from THO mice homed more efficiently to lymph nodes than their control counterparts, a pattern that mimicked the one observed for cells from desiccating stress mice(53) and that could be ascribed to the increased number of memory T cells in THO mice (Figure 1D). Three days after transfer, however, there was no difference in CD4+ T cell homing to cervical lymph nodes between THO recipients that were kept under normal conditions or subjected to desiccating stress. Nonetheless, THO recipients under desiccating stress developed a gradual reduction in tear production that was detectable from day 10 onwards (Figure 5C). Also, on day 16 after transfer, THO recipients showed corneal surface damage and increased irregularity (Figure 5D), two clinical signs of DED that are reproduced in the murine desiccating stress model(31,53). These effects were not observed in mice that were transferred with control cells and were kept under the same environmental conditions. Altogether these results show that the T cell response initiated by the disruptive effect of hyperosmolar stress on the ocular surface is sufficient to induce DED under mild desiccating stress.

Discussion

This study shows that tear film hyperosmolarity (THO) is sufficient to disrupt the neuroimmune homeostasis of the ocular surface. Specifically, we observed that THO modifies the way a surrogate antigen is handled by the ocular mucosal surface, from the basal-state tolerogenic response to an actual proinflammatory and potentially pathogenic T cell response. Also, THO induced changes in corneal intraepithelial nerve morphology and increased sensitivity to physical stimuli. Finally, the T cell response initiated by THO, although insufficient to induce corneal damage per se, did accelerate the course of the disease when transferred to mice under desiccating stress. All these findings highlight the pivotal role of THO in DED onset, and at the same time, provide clues on how two seemingly different aspects of DED, ocular surface inflammation and neuropathic pain, might be related.

Although the role of the adaptive immune response in DED pathophysiology is firmly established(43,52–54), the actual, either self- or non-self-derived ocular surface antigens involved remain unknown(17). This limitation, which precludes direct exploration of antigen-specific immune responses, was overcome in our model by imbibing the ocular surface with an exogenous inert antigen. Thus, we probed the physiological response to it, i.e. mucosal tolerance, as a substitute for immune homeostasis(18,19). In our study, the change in the way the ocular mucosal immune system ultimately reacts against a surrogate antigen was observed after three days of exposure to hyperosmolar stress, suggesting that immunogenic conditioning of the ocular surface must take place before this event. Luo et al(5) have previously shown in a similar in vivo model that hyperosmolar stress rapidly induces proinflammatory changes in murine corneal and conjunctival epithelial cells, namely activation of mitogen-activated protein kinase (MAPK) cascades and increased production of interleukin 1β, tumor necrosis factor α and matrix-associated metalloproteinase 9. The complete chain of events triggered by hyperosmolar stress on ocular surface epithelial cells remains unknown, but at least TRPV1 signaling pathway activation has been reported(49,50). In cultured corneal epithelial cells, hyperosmolar stress is sensed by TRPV1 channels, leading to Ca2+ transients and transactivation of the epidermal growth factor receptor; MAPK signaling then ensues, with subsequent NF-κB activation and increased IL-6 and IL-8 secretion(50). Interestingly, topical TRPV1 inhibition in our model also prevented the immune response towards OVA, supporting the role of this

signaling pathway in the early events induced by hyperosmolar stress. Also, we have previously described the key role of NF-κB activation in ocular surface epithelial cells for the conditioning of the subsequent steps in the mucosal immune response to an antigen(17,20–22,27), and in line with this, there was increased conjunctival epithelial NF-κB activity in mice exposed to THO in this model. More importantly, topical inhibition of NF-κB activation was sufficient to prevent mucosal tolerance disruption in the context of THO, underscoring the aforementioned dependence on this signaling pathway.

There are several reports of corneal nerve abnormalities detected by in vivo confocal microscopy and decreased corneal sensitivity in DED patients(24–26). It remains to be established whether these changes represent a core pathophysiological mechanism of DED or an epiphenomenon associated with ocular surface inflammation(28). Corneal DCs and sensory nerves are both structurally and functionally interdependent in mice(55,56). Remarkably, in our model THO also increased conjunctival DC number and activation and reduced corneal nerve density. In patients with infectious keratitis, corneal nerve density decreases as DC density increases irrespective of the duration of the disease(57), suggesting that these changes occur early and rapidly, as in our model. Interestingly, sensory nerve endings in the skin detect allergen through their TRPV1 receptors and, by releasing substance P, recruit DCs(58). Also, there is evidence of direct neurotoxicity induced by hyperosmolar tears on corneal nerve morphology and electrophysiological responses in rats(59). The effect is detectable within minutes of continuous exposure of the ocular surface to hyperosmolar solutions, causing degeneration of subbasal nerve fibers after several hours but no changes in intraepithelial nerve terminals. Such speed is surprising, hence the alleged neurotoxicity of hyperosmolar stress(59), which would be similar to the excitotoxicity mechanism already described for capsaicin- or glutamate-induced neuron death that involves overly intense receptor activation and cation entry(60,61). In DED patients, such prolonged exposure to hyperosmolar stress is unlikely because of blinking, but intermittently high osmolarity is predicted to occur(4,37,38,62). By contrast, our model involves repeated exposure of the ocular surface to hyperosmolar stress throughout the day, which could explain the differences in some of the findings. After five days of hyperosmolar stress, we also observed changes in superficial nerve terminals, with evidence of sensitization to THO. In an acute DED model, a similar decrease in intraepithelial corneal nerves was reported after five days of

desiccating stress, accompanied by the corresponding reduction in mechanical sensitivity(32). Perhaps the earliest changes in corneal nerve morphology and function are directly induced by THO, and later on in the course of DED, ocular surface inflammation induces additional neural dysfunction. At any rate, our findings support the idea that hyperosmolar stress affects intraepithelial corneal nerves, and since there is extensive neuroregulation of the ocular surface's immune homeostasis(27–29), this might contribute to the observed proinflammatory response towards an exogenous antigen.

Noteworthy, in our model, hyperosmolar stress was insufficient to induce clinically evident corneal epithelial damage, a hallmark of DED, when exerted on the ocular surface of mice for five days. By contrast, most murine DED models show manifest corneal fluorescein staining after a comparable time(21,22), and this could be ascribed to the stronger environmental challenge that desiccating stress represents compared to hyperosmolar stress. It should be noted that desiccating stress necessarily encompasses THO as a consequence of increased tear evaporation(63), and whereas desiccating stress is exerted for hours every day or continuously in these models, hypertonic saline instillation should only increase tear osmolarity temporarily. Despite the lack of overt clinical signs, two ocular surface changes that are associated with the early phase of DED are present in this model: disrupted immune homeostasis (as evidenced by loss of tolerance to a harmless exogenous antigen) and corneal nerve pathology (i.e. structural and functional changes). Intriguingly, T cells taken from mice after five days of hyperosmolar stress homed more efficiently to the eye-draining lymph nodes and worsened clinical DED signs in naïve recipients under mild desiccating stress. This finding suggests that the earliest events in the generation of the pathogenic T cell response that drives ocular surface damage in DED are already in motion in this THO model, albeit subclinically. It is unclear whether this represents T cells specific for an ocular surface autoantigen or a microbiome/exogenous antigen-oriented T cell response(17).

In summary, this murine model offers a unique opportunity to study the early events in DED pathogenesis that are triggered by THO. In humans, tear osmolarity, and therefore also hyperosmolar stress, fluctuate with blink rate and environmental conditions(4,64), perhaps more so with vocational or recreational video display and smartphone use(13). Other well-characterized murine DED models involve either semi-permanent or permanent ocular surface desiccation by abolishing tear secretion by pharmacological or surgical means(22,52). We believe this THO model better represents the

intermittent exposure to harsh ambient conditions that affects some DED patients, and although it is milder than the desiccating stress-based DED models, it still recapitulates most of the features of the disease. At any rate, this THO-induced neuroimmune disturbance could be useful for exploring novel therapeutic approaches targeted at the first steps in the escalating continuum of DED pathophysiology.

Materials and Methods

Mice. Balb/c (BALB/cAnNCrl) and C57BL/6 (C57BL/6NCrl) mice were originally obtained from Charles River Laboratories (Wilmington, MA, USA), whereas DO11.10 mice (C.Cg-Tg(DO11.10)10Dlo/J, JAX stock #003303) were from The Jackson Laboratory (Bar Harbor, ME, USA). Mice were bred and maintained at the Institute of Experimental Medicine conventional animal facility. All mice were 6-8 weeks old at the beginning of the experiments, and all protocols were approved by the Institute of Experimental Medicine animal ethics committee and adhered to the Association for Research in Vision and Ophthalmology Statement for the Use of Animals in Ophthalmic and Vision Research.

Reagents, antibodies, and cell cultures. All chemical and biological reagents were from Sigma-Aldrich (Buenos Aires, Argentina) unless otherwise specified. Grade V ovalbumin (OVA) was used in all experiments. A TRPV1 antagonist (SB-366791, CAS number: 472981-92-3) was included in some experiments. Fluorochrome-tagged antibodies were from BioLegend (San Diego, CA, USA) unless otherwise specified. All cell cultures were done in RPMI-1640 medium supplemented with 10% fetal calf serum, 10 mM glutamine, 100 U/ml penicillin, 100 μg/ml streptomycin, and $5x10^{-5}$ M 2-mercaptoethanol in a humidified incubator with 5% CO_2 at 37°C.

Mouse model of hyperosmolar stress. Mice were instilled 4 times/day on both eyes with 5 μl/eye of either isotonic phosphate-buffered saline (PBS) (isoosmolar treatment, 0.3 Osm/l, pH 7.4) or hypertonic PBS (prepared in deionized water from the same concentrated 10X stock solution used to prepare the isoosmolar solution: 3-fold dilution ~ 0.9 Osm/l, and undiluted -3 Osm/l-, both pH 7.4). For some experiments, mice also received 4 instillations/day on both eyes of either 100 μg/ml SB-366791 (TRPV1 antagonist) or 0.1 mM pyrrolidine dithiocarbamate at least 10 min before each instillation of isotonic or hypertonic PBS.

Ocular instillation of OVA, immunization for delayed-type hypersensitivity (DTH) assays, and in vitro antigen-specific T cell proliferation. For some experiments, mice were instilled twice daily at the indicated time points with 5 μl/eye of 2 mg/ml OVA as a surrogate ocular surface antigen. For the DTH assays, 0.1 ml of 1:1 PBS:complete Freund's adjuvant (CFA) emulsion containing 100 μg OVA were injected subcutaneously in the flank on day 8, and then on day 15, heat-aggregated OVA

(100 μg in PBS) and PBS alone were injected in a volume of 30 μl into the right and left footpads, respectively. Antigen-induced swelling was measured 48 h later with a dial thickness gauge as the mean difference in thickness between the right and left footpads of each mouse. For the in vitro assays, cervical, axillary, and inguinal lymph nodes were harvested after euthanasia and rendered into a cell suspension by mechanical dissociation and sieving through plastic mesh. Cells from each mouse were labeled with CFSE Cell Division Tracker Kit (BioLegend, San Diego, CA, USA) as per the manufacturer's instructions and then cultured in U-bottom 96-well plates at a concentration of $1x10^6$ cells/ml for 3 days in the presence of 100 μg/ml OVA. At the end of the culture period, cells were analyzed by flow cytometry.

Collection of eye tissue and cells from eye-draining lymph nodes. After euthanasia, the entire eye globe with the tarsal conjunctiva still attached was excised with the aid of a dissection microscope, and then the conjunctivas and corneas were dissected apart. The conjunctivas were fixed with 4% paraformaldehyde and the corneas were fixed with cold methanol before processing for immunostaining. For analysis of eye-draining lymph node cells, submandibular lymph nodes were excised and rendered into a cell suspension as described above.

Immunostaining and flow cytometry. For antigen staining, cells were washed in PBS with 0.5% BSA, incubated for 15 minutes with 5 μg/ml 2.4G2 antibody (purified from ascites fluid) to block non-specific binding to Fc receptors and then labeled with fluorochrome-conjugated antibodies for 30 minutes at 4°C. For flow cytometry analysis, cells were washed in PBS with 1 mM EDTA before acquisition on a Partec CyFlow Space cytometer (Sysmex Partec GmbH, Görlitz, Germany). Data was analyzed with Flowing Software (Perttu Terho, Centre for Biotechnology, Turku, Finland; www.flowingsoftware.com). Optimal compensation and gain settings, as well as viable cell gating, were determined as described previously(22).

Immunostaining and confocal laser scanning microscopy acquisition. After fixation for 1 h, the conjunctivas were permeabilized with PBS+Triton X-100 0.1% for 1 h and blocked with BSA 1% in PBS for 1 h at room temperature. For NFκB p65 quantification, the samples were processed as described previously(27). For DC quantification, samples were incubated overnight at 4°C with 2.5 ug/ml Alexa Fluor 488 anti-mouse I-A/I-E antibody (#107616, BioLegend, San Diego, CA, USA),

washed twice, and finally incubated with 1 μM ToPro-3 (ThermoFisher Scientific) for 30 min at 4° C for nuclear staining. For corneal nerve staining, samples were incubated with 20 mM EDTA at 37° C for 1 h, then incubated overnight at 4° C in PBS+Triton X-100 0.3%+BSA 1% in the presence of 2.5 ug/ml Alexa Fluor 488 anti-tubulin β3 antibody (#801203, BioLegend, San Diego, CA, USA), washed twice, and finally labeled with ToPro-3 as for DC quantification. In all cases, specimens were washed and mounted with Aqua-Poly/Mount medium and stored at 4° C. Image acquisition was performed by a masked observer with a FluoView FV1000 confocal microscope (Olympus, Tokyo, Japan) equipped with Plapon 60X/1.42 and UPlanSapo 20X/0.75 objectives. For NFκB p65 quantification, image acquisition and analysis were done as described previously(27). For corneal nerve and conjunctival DC image acquisition, a Z-stack scan (0.5-1 μm step size) was performed from the superficial epithelium to the corneal stroma (one central and three peripheral corneal scans) or the conjunctival lamina propria (three to five non-overlapping scans per sample). For all image analyses, ImageJ software was used (http://imagej.nih.gov/ij/ provided by the National Institutes of Health, Bethesda, MD, USA) by a masked observer.

DC image analysis. For DC density quantification, a maximum intensity Z-projection was created spanning the entire epithelium, then a 50-pixel rolling ball background correction (ImageJ) was applied, and finally, the DCs were counted manually. For DC field area quantification, one slice of the Z-stack was randomly chosen and a 15-pixel rolling ball background correction was applied. Then, the field area (dendrite tip to tip) of up to 10 DCs per image was determined using the Polygons Selections tool in Image J. Cells were randomly selected starting from the top left corner, as described by De Silva et al(33). For dendrite quantification, up to 10 DCs per image were similarly selected from the same images, and the dendrites were counted manually.

Corneal nerve image analysis. We followed the methods validated previously by others(32,33). For subbasal nerve quantification in the central corneal, Sholl analysis was applied using the corresponding ImageJ plugin. A maximal intensity Z-projection of the 3-5 slices spanning the basal corneal epithelial cells was created, then 50-pixel rolling ball background correction was applied, and finally, 12 concentric circles with a 10 μm radius step size were traced onto it; the results are expressed as the mean number of intersections of $TUBB3^{+}$ nerves in each concentric circle(32). For peripheral subbasal nerve quantification, Z-projections were created in the same way, converted to 8-

bit grayscale images, and analyzed by the Sum Length function of the NeuronJ plugin for ImageJ. To quantify intraepithelial nerve terminals, a single frame corresponding to the mid-epithelial layer was selected, containing only vertical projections of the axons. Then, background correction was applied, and finally, the axons were counted with the Cell Counter plugin for ImageJ.

Conjunctival transfer of BMDCs and allogeneic DTH assay. BMDCs were generated from bone marrow cultures of C57/BL6 or BALB/c mice in the presence of 20 ng/ml GM-CSF (PeproTech, Rocky Hill, NJ, USA) for 7 days, then nonadherent and loosely adherent cells were harvested as BMDCs. The purity of the DCs, determined by flow cytometry analysis of surface CD11c and MHC II staining, was >80%. In some experiments, OVA 100 μg/ml was added during the last 18 h of culture. Recipient mice were anesthetized with ketamine/xylazine, and then $5x10^5$ DCs/30 μl PBS were injected into the subconjunctival space through a 30G needle under a surgical microscope. For the allogeneic challenge, $5x10^5$ mitomycin-C treated allogeneic splenocytes/30 μl PBS were injected in the footpad, as described for the OVA challenge.

Adoptive transfer of DO11.10 T cells. CD4+ cells were isolated with magnetic beads (Miltenyi Biotec, Buenos Aires, Argentina) from pooled splenocytes and lymph node cells from DO11.10 mice, and then transferred to recipient naïve Balb/c mice by intraperitoneal injection ($5x10^6$ cells/mouse) in 0.5 ml PBS. Later, recipient mice were exposed to isoosmolar conditions or hyperosmolar stress for 5 days and received OVA in both eyes (5 μl/eye of 2 mg/ml OVA twice daily on days 4 and 5). Finally, mice were euthanatized and submandibular lymph nodes were excised to evaluate DO11.10+ T cell homing by flow cytometry. For some experiments, inguinal lymph nodes were also collected as controls.

Eyeblink test. Blinking was measured by restraining the mice mildly, to prevent them from wiping with the paws, and then applying 5 μl of 3X PBS (0.9 Osm/l) onto each eye. The blinking response was recorded for one minute, and the number of blinks was counted by two masked observers.

Adoptive transfer of T cells from THO mice. Splenocytes and lymph node cells were collected from mice exposed to isoosmolar or hyperosmolar treatment for 5 days, as described above, and then T cells were isolated by panning with B220 antibody. CD3+ T cells were >90% as assessed by flow cytometry. Naïve Balb/c mice that were administered 0.25 mg i.p. of CD25 antibody (purified from

PC61 hybridoma) 4 days before to deplete regulatory T cells were used as recipients and each mouse was injected i.p. with $15x10^6$ cells in 0.5 ml PBS. Recipient mice were housed in perforated cages to allow forced air to flow from a fan for 12 h a day (9 AM to 9 PM). For some experiments, T cells were labeled with CFSE as described above before the adoptive transfer.

Assessment of tear production and corneal surface damage and irregularity. Tear production was measured by wetting of phenol-red impregnated filter paper and corneal surface damage was assessed by fluorescein uptake, as described elsewhere(21,22). Corneal surface irregularity was determined by the reflection of an 8-white LED lamp array(31).

Statistical analysis. Student's *t*-test and one- or two-way analysis of variance (ANOVA) with Bonferroni post-hoc tests were used to compare means of two or more samples, respectively. Significance was set at $p<0.05$ and two-tailed tests were used in all experiments. Calculations were performed using GraphPad Prism version 7 software (GraphPad Software, La Jolla, Ca, USA).

Acknowledgments: None

Author contributions

Study conception and design: MG, JGG

Acquisition of data: MG, MM, IK, CMS, FS, FF, MNG, JGG

Analysis and interpretation of data: MG, MM, FF, MNG, AST, JGG

Drafting of manuscript: JGG

Critical revision: MG, MM, IK, CMS, FS, FF, MNG, AST, JGG

Funding sources: Agencia Nacional de Promoción Científica y Técnica, Argentina: FONCyT PICT 2013-1436, PICT 2015-0971, ARVO Roche Collaborative Research Fellowship

Conflict of interest: There is no conflict of interest for all the authors.

Data availability: The data that support the findings of this study are available from the corresponding author upon reasonable request.

References

1. Stapleton F, Alves M, Bunya VY, Jalbert I, Lekhanont K, Malet F, et al. TFOS DEWS II Epidemiology Report. Ocul Surf [Internet]. 2017 Jul [cited 2019 Jan 10];15(3):334–65. Available from: https://linkinghub.elsevier.com/retrieve/pii/S154201241730109X

2. Tomlinson A, Khanal S, Ramaesh K, Diaper C, McFadyen A. Tear film osmolarity: determination of a referent for dry eye diagnosis. Invest Ophthalmol Vis Sci [Internet]. 2006 Oct 1 [cited 2014 Nov 7];47(10):4309–15. Available from: http://www.ncbi.nlm.nih.gov/pubmed/17003420

3. Sullivan BD, Whitmer D, Nichols KK, Tomlinson A, Foulks GN, Geerling G, et al. An Objective Approach to Dry Eye Disease Severity. Investig Opthalmology Vis Sci [Internet]. 2010 Dec 1 [cited 2019 Jan 10];51(12):6125. Available from: http://www.ncbi.nlm.nih.gov/pubmed/20631232

4. Bron AJ, de Paiva CS, Chauhan SK, Bonini S, Gabison EE, Jain S, et al. TFOS DEWS II pathophysiology report. Ocul Surf [Internet]. 2017 Jul [cited 2019 Jan 10];15(3):438–510. Available from: http://www.ncbi.nlm.nih.gov/pubmed/28736340

5. Luo L, Li D-Q, Corrales RM, Pflugfelder SC. Hyperosmolar saline is a proinflammatory stress on the mouse ocular surface. Eye Contact Lens [Internet]. 2005 Sep [cited 2014 Oct 27];31(5):186–93. Available from: http://www.ncbi.nlm.nih.gov/pubmed/16163009

6. Li D-Q, Chen Z, Song XJ, Luo L, Pflugfelder SC. Stimulation of matrix metalloproteinases by hyperosmolarity via a JNK pathway in human corneal epithelial cells. Invest Ophthalmol Vis Sci [Internet]. 2004 Dec [cited 2013 Aug 29];45(12):4302–11. Available from: http://www.ncbi.nlm.nih.gov/pubmed/15557436

7. Luo L, Li D-Q, Pflugfelder SC. Hyperosmolarity-induced apoptosis in human corneal epithelial cells is mediated by cytochrome c and MAPK pathways. Cornea [Internet]. 2007 May [cited 2013 Jul 5];26(4):452–60. Available from: http://www.ncbi.nlm.nih.gov/pubmed/17457195

8. Li D-Q, Luo L, Chen Z, Kim H-S, Song XJ, Pflugfelder SC. JNK and ERK MAP kinases mediate induction of IL-1beta, TNF-alpha and IL-8 following hyperosmolar stress in human limbal epithelial cells. Exp Eye Res [Internet]. 2006 Apr [cited 2013 Aug 28];82(4):588–96. Available from: http://www.pubmedcentral.nih.gov/articlerender.fcgi?artid=2198933&tool=pmcentrez&rendertype=abstract

9. Kimura K, Teranishi S, Fukuda K, Kawamoto K, Nishida T. Delayed disruption of barrier function in cultured human corneal epithelial cells induced by tumor necrosis factor-alpha in a manner dependent on NF-kappaB. Invest Ophthalmol Vis Sci [Internet]. 2008 Feb [cited 2012 Oct 21];49(2):565–71. Available from: http://www.ncbi.nlm.nih.gov/pubmed/18235000

10. Argilés M, Cardona G, Pérez-Cabré E, Rodríguez M. Blink Rate and Incomplete Blinks in Six Different Controlled Hard-Copy and Electronic Reading Conditions. Investig Opthalmology Vis Sci [Internet]. 2015 Oct 15 [cited 2020 May 18];56(11):6679. Available from: http://iovs.arvojournals.org/article.aspx?doi=10.1167/iovs.15-16967

11. Wolkoff P. Eye complaints in the office environment: precorneal tear film integrity influenced by eye blinking efficiency. Occup Environ Med [Internet]. 2005 Jan 1 [cited 2020 May 18];62(1):4–12. Available from: http://oem.bmj.com/cgi/doi/10.1136/oem.2004.016030

12. Choi JH, Li Y, Kim SH, Jin R, Kim YH, Choi W, et al. The influences of smartphone use on the status of the tear film and ocular surface. PLoS One [Internet]. 2018 Oct 1 [cited 2020 Jun 10];13(10):e0206541. Available from: http://www.ncbi.nlm.nih.gov/pubmed/30379901

13. Yazici A, Sari ES, Sahin G, Kilic A, Cakmak H, Ayar O, et al. Change in tear film characteristics in visual display terminal users. Eur J Ophthalmol [Internet]. 25(2):85–9. Available from: http://www.ncbi.nlm.nih.gov/pubmed/25363850

14. Uchino M, Yokoi N, Uchino Y, Dogru M, Kawashima M, Komuro A, et al. Prevalence of Dry Eye Disease and its Risk Factors in Visual Display Terminal Users: The Osaka Study. Am J Ophthalmol [Internet]. 2013 Oct 1 [cited 2020 May 18];156(4):759-766.e1. Available from: https://www.sciencedirect.com/science/article/pii/S0002939413003838?casa_token=LV9zYsFNLPoAAAAA:JQT99ozXvKybda-VaHo3rEomahclhlMkHwZvUlK_gbnM1TAb3cNiK0aXb5ClG6TaqEivc4vYtaE

15. Coursey TG, Bohat R, Barbosa FL, Pflugfelder SC, de Paiva CS. Desiccating stress-induced chemokine expression in the epithelium is dependent on upregulation of NKG2D/RAE-1 and release of IFN-γ in experimental dry eye. J Immunol [Internet]. 2014 Nov 15 [cited 2015 Feb 27];193(10):5264–72. Available from: http://www.ncbi.nlm.nih.gov/pubmed/25288568

16. Zheng X, de Paiva CS, Li D-Q, Farley WJ, Pflugfelder SC. Desiccating stress promotion of Th17 differentiation by ocular surface tissues through a dendritic cell-mediated pathway. Invest Ophthalmol Vis Sci [Internet]. 2010 Jun 1 [cited 2012 Jul 15];51(6):3083–91. Available from: http://www.iovs.org/cgi/content/abstract/51/6/3083

17. Galletti JG, Guzmán M, Giordano MN. Mucosal immune tolerance at the ocular surface in health and disease. Immunology [Internet]. 2017 Apr [cited 2017 Jun 10];150(4):397–407. Available from: http://www.ncbi.nlm.nih.gov/pubmed/28108991

18. Egan RM, Yorkey C, Black R, Loh WK, Stevens JL, Storozynsky E, et al. In vivo behavior of

peptide-specific T cells during mucosal tolerance induction: antigen introduced through the mucosa of the conjunctiva elicits prolonged antigen-specific T cell priming followed by anergy. J Immunol [Internet]. 2000 May 1 [cited 2017 Feb 9];164,(9):4543–50. Available from: http://www.ncbi.nlm.nih.gov/pubmed/10779755

19. Galletti JG, Gabelloni ML, Morande PE, Sabbione F, Vermeulen ME, Trevani AS, et al. Benzalkonium chloride breaks down conjunctival immunological tolerance in a murine model. Mucosal Immunol [Internet]. 2013 Jan [cited 2013 Jun 7];6(1):24–34. Available from: http://www.ncbi.nlm.nih.gov/pubmed/22692451

20. Guzmán M, Sabbione F, Gabelloni ML, Vanzulli S, Trevani AS, Giordano MN, et al. Restoring conjunctival tolerance by topical nuclear factor-κB inhibitors reduces preservative-facilitated allergic conjunctivitis in mice. Invest Ophthalmol Vis Sci [Internet]. 2014 Sep 4 [cited 2016 Aug 10];55(9):6116–26. Available from: http://www.ncbi.nlm.nih.gov/pubmed/25190648

21. Guzmán M, Keitelman I, Sabbione F, Trevani AS, Giordano MN, Galletti JG. Desiccating stress-induced disruption of ocular surface immune tolerance drives dry eye disease. Clin Exp Immunol [Internet]. 2016 May 21 [cited 2016 Jan 4];184(2):248–56. Available from: http://www.ncbi.nlm.nih.gov/pubmed/26690299

22. Guzmán M, Keitelman I, Sabbione F, Trevani AS, Giordano MN, Galletti JG. Mucosal tolerance disruption favors disease progression in an extraorbital lacrimal gland excision model of murine dry eye. Exp Eye Res [Internet]. 2016 Oct [cited 2016 Jul 27];151:19–22. Available from: http://linkinghub.elsevier.com/retrieve/pii/S0014483516301798

23. Z H, A T. Gene Induction by Desiccation Stress in Human Cell Cultures. FEBS Lett [Internet]. 2005 [cited 2020 May 19];579(22). Available from: https://pubmed.ncbi.nlm.nih.gov/16115627/

24. Galor A, Moein H-R, Lee C, Rodriguez A, Felix ER, Sarantopoulos KD, et al. Neuropathic pain and dry eye. Ocul Surf [Internet]. 2018 Jan [cited 2019 Jan 3];16(1):31–44. Available from: http://www.ncbi.nlm.nih.gov/pubmed/29031645

25. Tuominen ISJ, Konttinen YT, Vesaluoma MH, Moilanen JAO, Helinto¨ M, Tervo TMT. Corneal Innervation and Morphology in Primary Sjögren's Syndrome. Investig Opthalmology Vis Sci [Internet]. 2003 Jun 1 [cited 2020 Feb 19];44(6):2545. Available from: http://www.ncbi.nlm.nih.gov/pubmed/12766055

26. del Castillo JMB, Wasfy MAS, Fernandez C, Garcia-Sanchez J. An In Vivo Confocal Masked Study on Corneal Epithelium and Subbasal Nerves in Patients with Dry Eye. Investig Opthalmology Vis Sci [Internet]. 2004 Sep 1 [cited 2020 Feb 19];45(9):3030. Available from: http://www.ncbi.nlm.nih.gov/pubmed/15326117

27. Guzmán M, Miglio MSMS, Zgajnar NRNR, Colado A, Almejún MBMB, Keitelman IAIAIA, et al. The mucosal surfaces of both eyes are immunologically linked by a neurogenic inflammatory reflex involving TRPV1 and substance P. Mucosal Immunol [Internet]. 2018 Jun 4 [cited 2018 Jun 6];11(5):1441–53. Available from: http://www.ncbi.nlm.nih.gov/pubmed/29867077

28. Labetoulle M, Baudouin C, Calonge M, Merayo-Lloves J, Boboridis KG, Akova YA, et al. Role of corneal nerves in ocular surface homeostasis and disease. Acta Ophthalmol [Internet]. 2019 Mar [cited 2020 Feb 20];97(2):137–45. Available from: http://www.ncbi.nlm.nih.gov/pubmed/30225941

29. Foulsham W, Coco G, Amouzegar A, Chauhan SK, Dana R. When Clarity Is Crucial: Regulating Ocular Surface Immunity. Trends Immunol [Internet]. 2018 [cited 2020 Feb 20];39(4):288–301. Available from: http://www.ncbi.nlm.nih.gov/pubmed/29248310

30. Marfurt CF, Cox J, Deek S, Dvorscak L. Anatomy of the human corneal innervation. Exp Eye Res [Internet]. 2010 Apr [cited 2018 Aug 19];90(4):478–92. Available from: http://www.ncbi.nlm.nih.gov/pubmed/20036654

31. De Paiva CS, Corrales RM, Villarreal AL, Farley W, Li D-Q, Stern ME, et al. Apical corneal barrier disruption in experimental murine dry eye is abrogated by methylprednisolone and doxycycline. Invest Ophthalmol Vis Sci [Internet]. 2006 Jul 1 [cited 2014 Dec 25];47(7):2847–56. Available from: http://www.iovs.org/content/47/7/2847.long

32. Stepp MA, Pal-Ghosh S, Tadvalkar G, Williams A, Pflugfelder SC, de Paiva CS. Reduced intraepithelial corneal nerve density and sensitivity accompany desiccating stress and aging in C57BL/6 mice. Exp Eye Res [Internet]. 2018 [cited 2020 Feb 20];169:91–8. Available from: http://www.ncbi.nlm.nih.gov/pubmed/29407221

33. De Silva MEH, Hill LJ, Downie LE, Chinnery HR. The Effects of Aging on Corneal and Ocular Surface Homeostasis in Mice. Investig Opthalmology Vis Sci [Internet]. 2019 Jun 26 [cited 2020 May 19];60(7):2705. Available from: http://iovs.arvojournals.org/article.aspx?doi=10.1167/iovs.19-26631

34. Willcox MDP, Argüeso P, Georgiev GA, Holopainen JM, Laurie GW, Millar TJ, et al. TFOS DEWS II Tear Film Report. Ocul Surf [Internet]. 2017 Jul 1 [cited 2020 Jun 22];15(3):366–403. Available from: /pmc/articles/PMC6035753/?report=abstract

35. Gaffney EAA, Tiffany JMM, Yokoi N, Bron AJJ. A mass and solute balance model for tear volume and osmolarity in the normal and the dry eye. Prog Retin Eye Res [Internet]. 2010 Jan [cited 2014 Nov 13];29(1):59–78. Available from: https://linkinghub.elsevier.com/retrieve/pii/S1350946209000718

36. Chen Q, Wang J, Tao A, Shen M, Jiao S, Lu F. Ultrahigh-Resolution Measurement by Optical Coherence Tomography of Dynamic Tear Film Changes on Contact Lenses. Invest Ophthalmol Vis Sci [Internet]. 2010 [cited 2020 May 6];51(4):1988. Available from: https://www.ncbi.nlm.nih.gov/pmc/articles/PMC2868399/

37. Liu H, Begley C, Chen M, Bradley A, Bonanno J, McNamara NA, et al. A link between tear instability and hyperosmolarity in dry eye. Invest Ophthalmol Vis Sci [Internet]. 2009 Aug 1 [cited 2014 Oct 20];50(8):3671–9. Available from: http://iovs.arvojournals.org/article.aspx?doi=10.1167/iovs.08-2689

38. Braun RJ, King-Smith PE, Begley CG, Li L, Gewecke NR. Dynamics and function of the tear film in relation to the blink cycle. Prog Retin Eye Res [Internet]. 2015 Mar;45:132–64. Available from: http://www.ncbi.nlm.nih.gov/pubmed/25479602

39. Pabst O, Mowat AM. Oral tolerance to food protein. Mucosal Immunol [Internet]. 2012 May 8

[cited 2014 Oct 30];5(3):232–9. Available from: http://dx.doi.org/10.1038/mi.2012.4

40. Zhang X, Schaumburg CS, Coursey TG, Siemasko KF, Volpe EA, Gandhi NB, et al. $CD8^+$ cells regulate the T helper-17 response in an experimental murine model of Sjögren syndrome. Mucosal Immunol [Internet]. 2014 Mar [cited 2014 Oct 14];7(2):417–27. Available from: http://www.pubmedcentral.nih.gov/articlerender.fcgi?artid=3869878&tool=pmcentrez&rendertype=abstract

41. Swamy M, Jamora C, Havran W, Hayday A. Epithelial decision makers: in search of the "epimmunome." Nat Immunol [Internet]. 2010;11,:656–65. Available from: http://dx.doi.org/10.1038/ni.1905

42. Ather JL, Foley KL, Suratt BT, Boyson JE, Poynter ME. Airway epithelial NF-κB activation promotes the ability to overcome inhalational antigen tolerance. Clin Exp Allergy [Internet]. 2015 Jul [cited 2017 Dec 22];45(7):1245–58. Available from: http://www.ncbi.nlm.nih.gov/pubmed/25616105

43. Schaumburg CS, Siemasko KF, De Paiva CS, Wheeler LA, Niederkorn JY, Pflugfelder SC, et al. Ocular surface APCs are necessary for autoreactive T cell-mediated experimental autoimmune lacrimal keratoconjunctivitis. J Immunol [Internet]. 2011 Oct 1 [cited 2015 Jul 18];187(7):3653–62. Available from: http://www.ncbi.nlm.nih.gov/pubmed/21880984

44. Lee HS, Amouzegar A, Dana R. Kinetics of Corneal Antigen Presenting Cells in Experimental Dry Eye Disease. BMJ open Ophthalmol [Internet]. 2017 [cited 2020 Mar 15];1(1):e000078. Available from: http://www.ncbi.nlm.nih.gov/pubmed/29354712

45. Wakamatsu TH, Sato EA, Matsumoto Y, Ibrahim OMA, Dogru M, Kaido M, et al. Conjunctival in vivo confocal scanning laser microscopy in patients with Sjögren syndrome. Invest Ophthalmol Vis Sci [Internet]. 2010 Jan [cited 2020 Jun 6];51(1):144–50. Available from: http://www.ncbi.nlm.nih.gov/pubmed/19696170

46. Kheirkhah A, Rahimi Darabad R, Cruzat A, Hajrasouliha AR, Witkin D, Wong N, et al. Corneal Epithelial Immune Dendritic Cell Alterations in Subtypes of Dry Eye Disease: A Pilot In Vivo Confocal Microscopic Study. Invest Ophthalmol Vis Sci [Internet]. 2015 Nov [cited

2020 Jun 6];56(12):7179–85. Available from: http://www.ncbi.nlm.nih.gov/pubmed/26540656

47. Aggarwal S, Kheirkhah A, Cavalcanti BM, Cruzat A, Jamali A, Hamrah P. Correlation of corneal immune cell changes with clinical severity in dry eye disease: An in vivo confocal microscopy study. Ocul Surf [Internet]. 2020; Available from: http://www.sciencedirect.com/science/article/pii/S1542012420300963

48. Maruoka S, Inaba M, Ogata N. Activation of Dendritic Cells in Dry Eye Mouse Model. Investig Opthalmology Vis Sci [Internet]. 2018 Jul 2 [cited 2020 Mar 15];59(8):3269. Available from: http://iovs.arvojournals.org/article.aspx?doi=10.1167/iovs.17-22550

49. Hua X, Su Z, Deng R, Lin J, Li D-Q, Pflugfelder SC. Effects of L-carnitine, erythritol and betaine on pro-inflammatory markers in primary human corneal epithelial cells exposed to hyperosmotic stress. Curr Eye Res [Internet]. 2015 Jul [cited 2020 Jan 23];40(7):657–67. Available from: http://www.ncbi.nlm.nih.gov/pubmed/25271595

50. Pan Z, Wang Z, Yang H, Zhang F, Reinach PS. TRPV1 activation is required for hypertonicity-stimulated inflammatory cytokine release in human corneal epithelial cells. Invest Ophthalmol Vis Sci [Internet]. 2011 Jan [cited 2020 Jan 23];52(1):485–93. Available from: http://www.ncbi.nlm.nih.gov/pubmed/20739465

51. Galor A. Painful Dry Eye Symptoms: A Nerve Problem or a Tear Problem? Ophthalmology [Internet]. 2019 May [cited 2020 Mar 16];126(5):648–51. Available from: http://www.ncbi.nlm.nih.gov/pubmed/31005185

52. Niederkorn JY, Stern ME, Pflugfelder SC, De Paiva CS, Corrales RM, Gao J, et al. Desiccating stress induces T cell-mediated Sjögren's Syndrome-like lacrimal keratoconjunctivitis. J Immunol [Internet]. 2006 Apr 1 [cited 2012 Sep 11];176(7):3950–7. Available from: http://www.ncbi.nlm.nih.gov/pubmed/16547229

53. Chen Y, Chauhan SK, Lee HS, Saban DR, Dana R. Chronic dry eye disease is principally mediated by effector memory Th17 cells. Mucosal Immunol [Internet]. 2014 Jan [cited 2014 Mar 28];7(1):38–45. Available from: http://dx.doi.org/10.1038/mi.2013.20

54. Kodati S, Chauhan SK, Chen Y, Dohlman TH, Karimian P, Saban D, et al. CCR7 is critical for the induction and maintenance of Th17 immunity in dry eye disease. Invest Ophthalmol Vis Sci [Internet]. 2014 Sep 18 [cited 2015 Mar 27];55(9):5871–7. Available from: http://www.pubmedcentral.nih.gov/articlerender.fcgi?artid=4168741&tool=pmcentrez&rendertype=abstract

55. Jamali A, Seyed-Razavi Y, Chao C, Ortiz G, Kenyon B, Blanco T, et al. Intravital Multiphoton Microscopy of the Ocular Surface: Alterations in Conventional Dendritic Cell Morphology and Kinetics in Dry Eye Disease. Front Immunol. 2020 May 7;11.

56. Gao N, Lee P, Yu F-S. Intraepithelial dendritic cells and sensory nerves are structurally associated and functional interdependent in the cornea. Sci Rep [Internet]. 2016 Dec 2 [cited 2018 Aug 24];6(1):36414. Available from: http://www.ncbi.nlm.nih.gov/pubmed/27805041

57. Cruzat A, Witkin D, Baniasadi N, Zheng L, Ciolino JB, Jurkunas U V., et al. Inflammation and the nervous system: The connection in the cornea in patients with infectious keratitis. Investig Ophthalmol Vis Sci. 2011 Jul;52(8):5136–43.

58. Aderhold PA, Dewan ZNA, Perner C, Flayer CH, Zhu X, Voisin T, et al. Allergen-induced dendritic cell migration is controlled through Substance P release by sensory neurons. bioRxiv [Internet]. 2020 Jan 1;2020.06.05.136929. Available from: http://biorxiv.org/content/early/2020/06/06/2020.06.05.136929.abstract

59. Hirata H, Mizerska K, Marfurt CF, Rosenblatt MI. Hyperosmolar Tears Induce Functional and Structural Alterations of Corneal Nerves: Electrophysiological and Anatomical Evidence Toward Neurotoxicity. Investig Opthalmology Vis Sci [Internet]. 2015 Dec 22 [cited 2020 Jan 2];56(13):8125. Available from: http://www.ncbi.nlm.nih.gov/pubmed/26720465

60. Pecze L, Blum W, Schwaller B. Mechanism of capsaicin receptor TRPV1-mediated toxicity in pain-sensing neurons focusing on the effects of Na+/Ca2+ fluxes and the Ca2+-binding protein calretinin. Biochim Biophys Acta - Mol Cell Res [Internet]. 2013 Jul [cited 2020 Feb 20];1833(7):1680–91. Available from: http://www.ncbi.nlm.nih.gov/pubmed/22982061

61. Faddis BT, Hasbani MJ, Goldberg MP. Calpain activation contributes to dendritic remodeling

after brief excitotoxic injury in vitro. J Neurosci [Internet]. 1997 Feb 1 [cited 2020 Feb 20];17(3):951–9. Available from: http://www.ncbi.nlm.nih.gov/pubmed/8994050

62. King-Smith PE, Nichols JJ, Nichols KK, Fink BA, Braun RJ. Contributions of Evaporation and Other Mechanisms to Tear Film Thinning and Break-Up. Optom Vis Sci [Internet]. 2008 Aug [cited 2020 Feb 20];85(8):623–30. Available from: http://www.ncbi.nlm.nih.gov/pubmed/18677230

63. McMonnies CW. Conjunctival Tear Layer Temperature, Evaporation, Hyperosmolarity, Inflammation, Hyperemia, Tissue Damage, and Symptoms: A Review of an Amplifying Cascade. Curr Eye Res [Internet]. 2017 Dec 2 [cited 2020 Mar 16];42(12):1574–84. Available from: http://www.ncbi.nlm.nih.gov/pubmed/29111837

64. Alex A, Edwards A, Hays JD, Kerkstra M, Shih A, de Paiva CS, et al. Factors predicting the ocular surface response to desiccating environmental stress. Invest Ophthalmol Vis Sci [Internet]. 2013 May 7 [cited 2016 Jul 29];54(5):3325–32. Available from: http://www.ncbi.nlm.nih.gov/pubmed/23572103

Figure legends

Figure 1 - THO disrupts mucosal immune homeostasis of the ocular surface. A) Experimental design for assessing the effect of hyperosmolar stress on ocular surface immune tolerance. Mice were instilled iso- (0.3 Osm/l) or hyperosmolar (0.9 and 3 Osm/l) saline on both eyes 4 times daily for 5 days, then immunized s.c. (Imm) with OVA+CFA and assayed one week later. OVA was instilled in both eyes on days 4 and 5 for experiments shown in B and C. **B)** In vivo DTH assay (OVA-induced footpad swelling) measured 48 h after challenge. Results are shown as the difference between the OVA-injected and PBS-injected footpads. **C)** In vitro CD4+ T cell proliferation of splenocytes harvested on day 15 and stimulated with OVA over a 4-day culture period, as assayed by CFSE dilution. Results are expressed relative to the proliferative fraction observed in control (immunized only) mice. **D)** FACS analysis of T cells obtained on day 5 from submandibular lymph nodes of control, isoosmolar and hyperosmolar treatment mice. *Data are expressed as mean ± SD (n=3-5 experiments, 3-5 mice/group). * indicates a statistically significant difference and ns a non-significant difference, as determined by ANOVA with Bonferroni's correction.*

Figure 2. THO modifies the ocular surface immune microenvironment. Mice were exposed to isoosmolar (0.3 Osm/l) or hyperosmolar (3 Osm/l) treatment for 3 days to allow for conditioning of the ocular surface to take place. **A)** Dot plot (left) and representative confocal micrographs (right) of nuclear localization of NF-κB p65 protein (red) relative to individual cell expression (green: phalloidin, blue: TO-PRO-3) in the conjunctival epithelium of isoosmolar and hyperosmolar treatment mice. Mean±SD of at least 200 cells analyzed from samples from 3 mice/group (representative example of 3 independent experiments). **B)** Effect of including the instillation of pyrrolidine dithiocarbamate (an NF-κB inhibitor) during hyperosmolar treatment as assessed by the in vivo DTH assay (OVA-induced footpad swelling). The experimental setup was already described in Figure 1B. Results are shown as the difference (mean±SD) between the OVA-injected and PBS-injected footpads. **C)** Cell density (left, mean±SD) and representative micrographs (right, calculated cell density on top), **D)** tree area (left, mean±SD) and representative micrographs (right), and **E)** number of dendrites (left, mean±SD) and representative micrographs (right) of conjunctival dendritic cells after 3 days of isoosmolar and hyperosmolar treatment (white: MHC II). **F)** In vivo DTH assay (allogeneic splenocyte-induced footpad swelling) measured 48 h after challenge of mice that were

subjected to iso- (0.3) or hyperosmolar (3) treatment for 3 days, then injected in the subconjunctival space of each eye with $5x10^5$ allogeneic BMDCs. Control (-) mice were injected with subconjunctival saline for reference and the DTH assay was performed one week later. Results are shown as the difference (mean±SD) between the splenocyte-injected and PBS-injected footpads. **G)** OVA-induced CD4+ T cell proliferation assayed by FACS (mean±SD, CFSE dye dilution) over a 4-day culture of submandibular lymph node cells from mice that were subjected to iso- (0.3) or hyperosmolar (3) treatment for 3 days, then injected in the subconjunctival space of each eye with $5x10^5$ OVA-pulsed syngeneic BMDCs and euthanized 4 days later. Mice injected with unloaded BMDCs (-) served as a reference. **H)** Homing of adoptively transferred CD4+/DO11.10+ T cells (mean±SD) to submandibular lymph nodes after 3 days of control, iso- (0.3) or hyperosmolar (3) treatment and OVA instillation. **I)** Effect of adding the instillation of a TRPV1 blocker during hyperosmolar treatment as assessed by the in vivo DTH assay (OVA-induced footpad swelling). The experimental setup was already described in Figure 1B. Results are shown as the difference (mean±SD) between the OVA-injected and PBS-injected footpads. *For all experiments, data are expressed as mean ± SD (n=3-5 experiments, 3-5 mice/group). * indicates a statistically significant difference and ns a non-significant difference, as determined by Student's t-test or ANOVA with Bonferroni's correction.*

Figure 3 – THO affects corneal intraepithelial nerves. Mice were exposed to isoosmolar (0.3 Osm/l) or hyperosmolar (3 Osm/l) treatment for 5 days before physiological testing and euthanasia. Corneal nerves were stained with an anti-tubulin β3 antibody. **A)** Quantification of intraepithelial nerve terminals (left) and representative images (right, green: tubulin β3). **B)** Quantification (Sholl analysis) of central subbasal nerve density (left, mean±SEM of nerve intersections for each concentric shell of specified radius) and representative images (right, white: tubulin β3). **C)** Quantification (sum length) of peripheral subbasal nerve density (left) and representative images (right green: tubulin β3). **D)** Blinking response to a hypertonic stimulus (number of blinks over one minute). *For all experiments, pooled data (mean ± SD unless otherwise specified) from two independent experiments, n=3-5 mice/group. * indicates a statistically significant difference, as determined by Student's t-test or two-factor ANOVA for Sholl analysis (treatment and radius).*

Figure 4 – Mice under THO for 5 days do not develop clinical signs of DED. Mice were exposed to isoosmolar (0.3 Osm/l, blue symbols) or hyperosmolar (3 Osm/l, red symbols) treatment for 5 days.

A) Tear production levels as assessed daily. **B)** Corneal fluorescein staining score (National Eye Institute scale, left panel) and representative photos taken on day 5 (right). **C)** Corneal irregularity score (left) and representative photos from day 5 (right). *Pooled data (mean±SD) from three independent experiments, 4-6 mice/group. ns indicates no statistically significant difference for treatment between groups by two-factor ANOVA (treatment and time).*

Figure 5 - THO initiates a T cell response that favors DED development. A) Experimental design: Mice were exposed to isoosmolar (0.3 Osm/l) or hyperosmolar (3 Osm/l) treatment for 5 days before T cell isolation and transfer to naïve recipients that were then exposed to mild desiccating stress (DS) and monitored for up to 16 days. **B)** T cells from isoosmolar (blue) or hyperosmolar (red) treatment mice were labeled with CFSE before transfer, and the eye-draining lymph nodes of the recipient mice were harvested 3 days after transfer. Proportion of transferred (CFSE+) T cells within the CD4+ and CD8+ populations in recipient mice housed under control conditions (filled bars) or mild desiccating stress (hatched bars). **C)** Tear production in isoosmolar (blue circles) and hyperosmolar (red squares) T cell recipients under desiccating stress. **D)** Representative photographs of corneal fluorescein staining and corneal surface irregularity assessments of T cell recipients under desiccating stress on day 16 after transfer. *Pooled data (mean±SD) of two independent experiments with 4-6 mice/group. * indicates a statistically significant difference, as determined by two-factor ANOVA (for B, osmolarity and DS; for C, osmolarity and time) with Bonferroni's correction.*

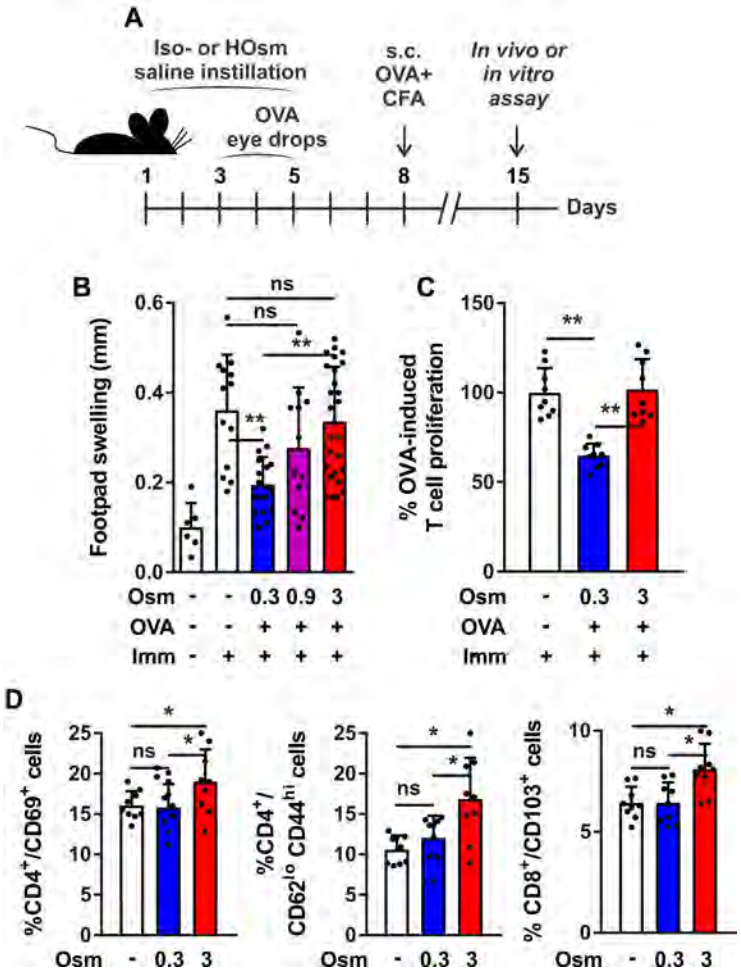

imm_13243_f1.png

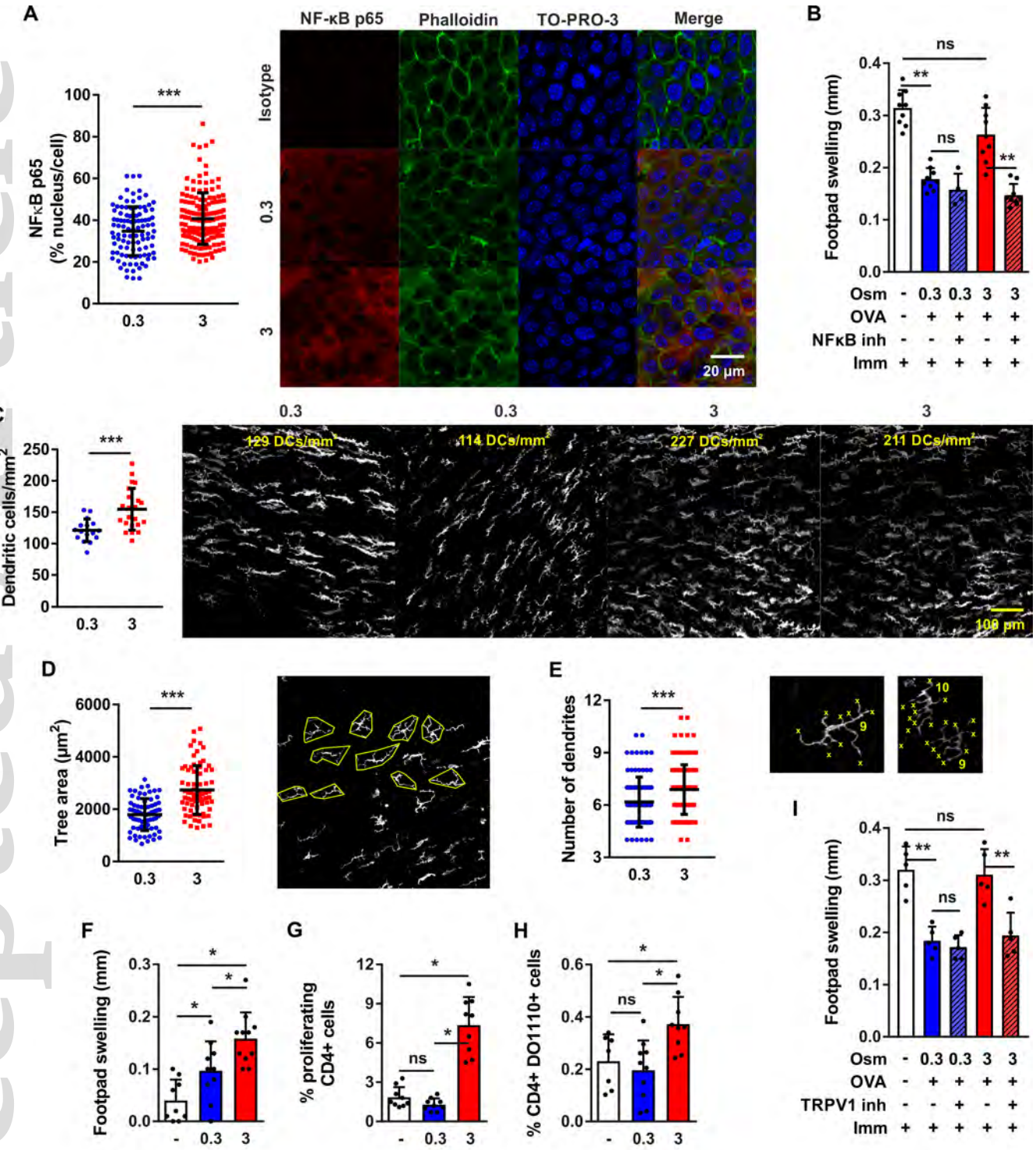

imm_13243_f2.png

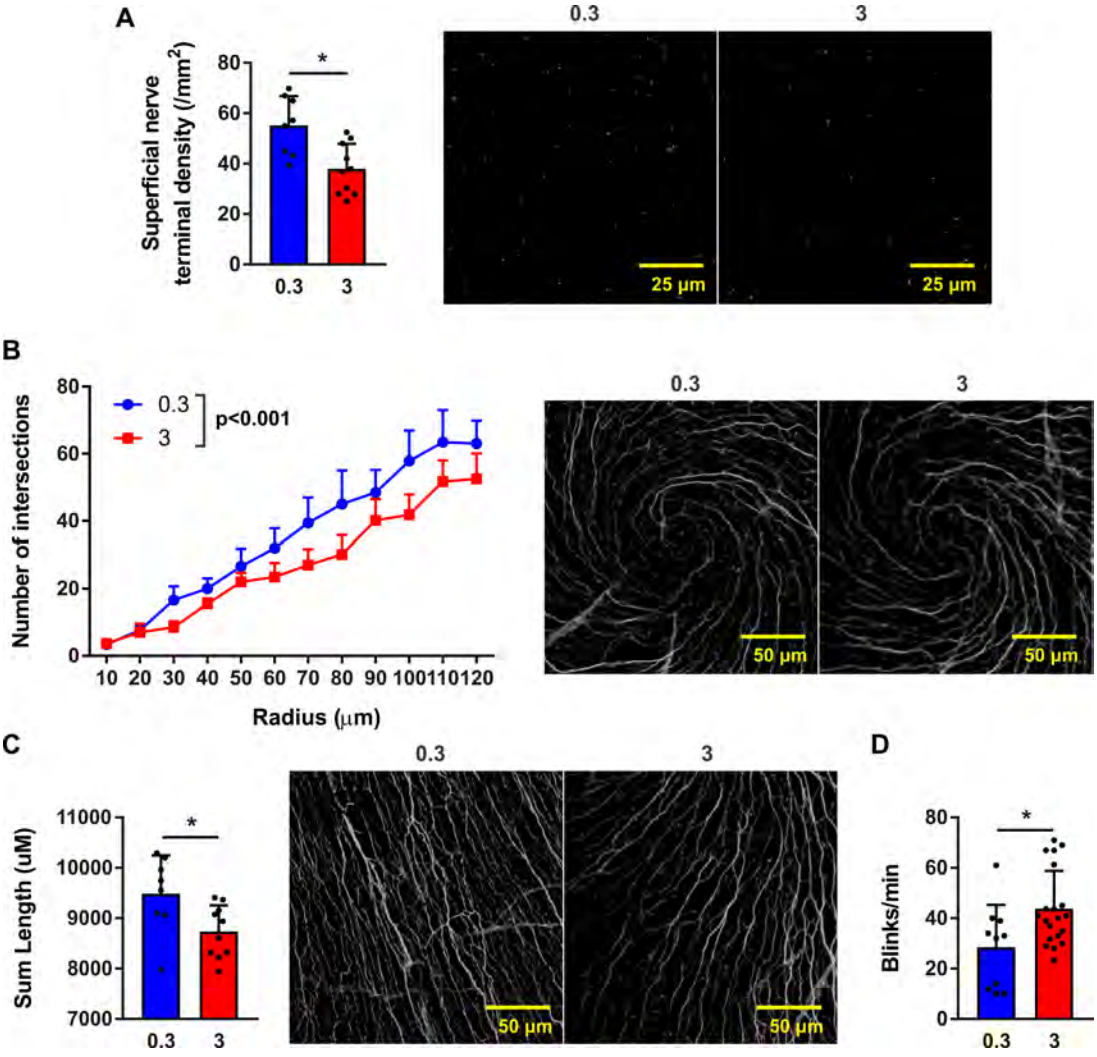

imm_13243_f3.png

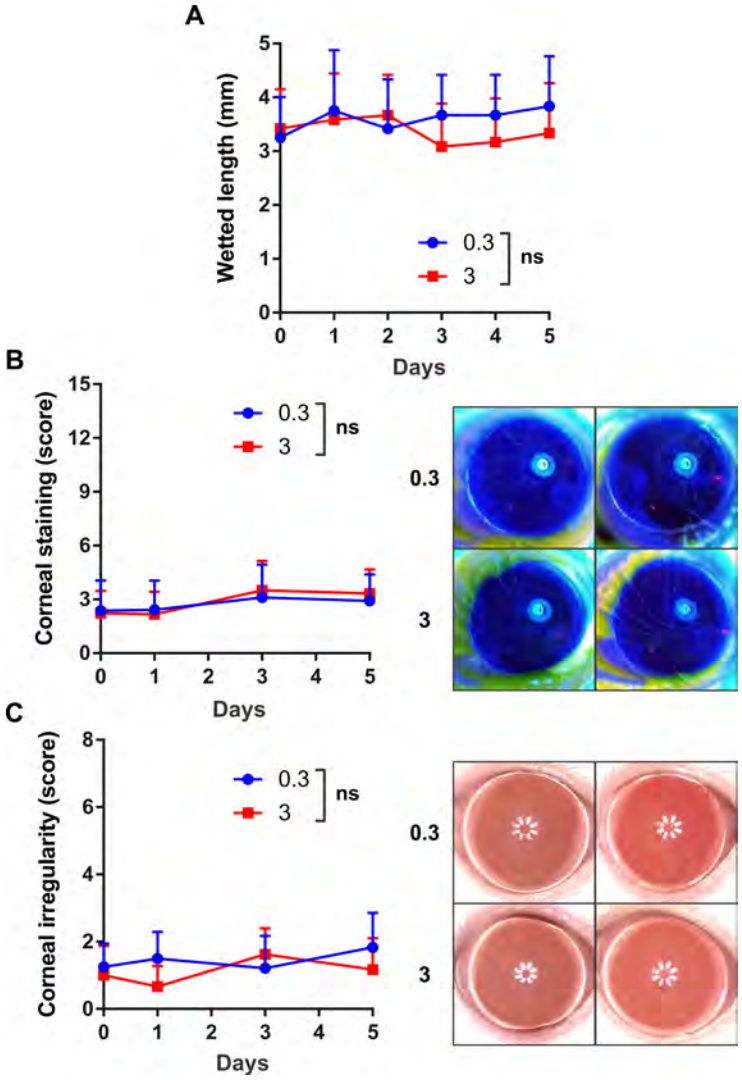

imm_13243_f4.png

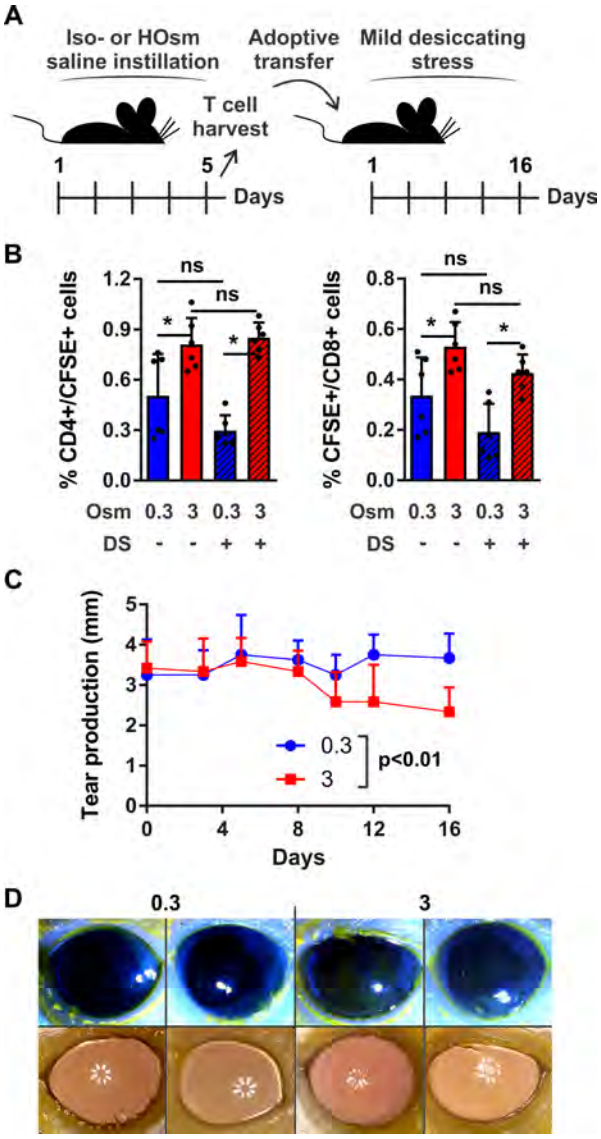

imm_13243_f5.png